Adaptive Prescribed Performance Motion Control of Servo Mechanisms with Friction Compensation

Jing Na, Qiang Chen, Xuemei Ren, and Yu Guo

***Abstract*—This paper proposes an adaptive control for a class of nonlinear mechanisms with guaranteed transient and steady-state performance. A performance function characterizing the convergence rate, maximum overshoot, and steady-state error is used for the output error transformation, such that stabilizing the transformed system is sufficient to achieve the tracking control of the original system with *a priori* prescribed performance. A continuously differentiable friction model is adopted to account for the friction nonlinearities, for which primary model parameters are online updated. A novel high-order neural network with only a scalar weight is developed to approximate unknown nonlinearities and to dramatically diminish the computational costs. Comparative experiments on a turntable servo system are included to verify the reliability and effectiveness.**

***Index Terms*—Adaptive control, friction compensation, motion control, neural networks (NNs), servo mechanisms.**

I. Introduction

In MODERN engineering systems, turntable servo mechanisms are widely used, where the presence of mechanical reduction and transmission devices (e.g., gears and lead screws) connected to actuators may introduce diverse nonlinearities, such as friction [1], dead zone [2], and disturbances. Among these dynamics, friction occurs unavoidably in various rotary mechanical systems and results in deteriorated performance or even limit cycles [3]. To eliminate the effects of friction and achieve highly precise motion control, significant effort has been devoted to build friction models that are capable of capturing different friction dynamics, e.g., classical model [4], Armstrong's model [5], Dahl model [6], and LuGre model [7]. With these friction models, some model-based compensation schemes have been proposed [1], [3], [8]. However, the precise modeling of friction is challenging and difficult as there are usually discontinuous dynamics embedded in these models so that time-consuming offline identification should be conducted to determine all model parameters *a priori*. Moreover, the fixed friction coefficients may not be able to account for time-varying friction dynamics over a wide operation range.

To accommodate time-varying dynamics, adaptive control [9] has been proven to be a powerful methodology for servo mechanisms [10]. In [11], proportional–integral–differential (PID) control was combined with an adaptive scheme to compensate for the modeling uncertainties. In [12], a disturbance observer was further incorporated into the adaptive control to handle time-varying disturbances. Xu *et al.* and Hu *et al.* proposed and experimentally validated the adaptive robust control (ARC) [13], [14] for precise motion control of servo systems with various dynamics (e.g., friction, force ripple, and dead zone). In subsequent work, an observer was employed to achieve output tracking control [15], and dynamic surface control (DSC) was utilized to remedy the "explosion of complexity" in backstepping control [16]. An identifier-based ARC scheme was proposed in [17], where a switching-logic-based adaptive law is presented. In aforementioned ARCs, a linearly parameterized friction model is employed to model Coulomb and viscous frictions. Although the offline identification of friction is avoided, the upper and lower bounds of unknown parameters are assumed to be known. Moreover, the studied systems are imposed to be in a linear-in-parameter form.

To handle unknown nonlinearities and disturbances, several nonlinear approximators, e.g., neural networks (NNs) and fuzzy systems, have been used. In [18] and [19], an adaptive feedforward NN control action was superimposed to feedback control to handle unknown nonlinearities, including friction, and experimental results on hard disk drives reveal the improved performance. In [20], a fuzzy NN was proposed for a two-axis motion control system. A composite adaptive law with both tracking error and predictor error was studied [21]. In these schemes, the friction is taken as a part of unknown nonlinearities to be approximated; thus, no precise friction model is required. However, the NN weights to be updated are either a vector or a matrix depending on the number of neurons, such that the subsequent computational costs may be demanding. Moreover, in all aforementioned control methods, the transient tracking performance cannot be quantitatively studied and/or prescribed designed. Guaranteeing tracking transient performance of system output response is an important but challenging task and an open problem in adaptive control. Recently, an attempt to establish *a priori* specified performance control paradigm has been exploited [22], [23], where the maximum overshoot, the convergence rate, and steady-state error are all addressed.

In this paper, we will propose an adaptive neural control for nonlinear servo mechanisms with prescribed transient and steady-state tracking performance. Inspired by [22] and [23], an

Manuscript received June 17, 2012; revised October 11, 2012; accepted December 24, 2012. Date of publication January 16, 2013; date of current version July 18, 2013. This work was supported by the National Natural Science Foundation of China under Grant 61203066, Grant 61273150, and Grant 60974046.

J. Na and Y. Guo are with the Faculty of Mechanical and Electrical Engineering, Kunming University of Science and Technology, Kunming 650093, China (e-mail: najing25@163.com).

Q. Chen is with the College of Information Engineering, Zhejiang University of Technology, Hangzhou 310023, China.

X. Ren is with the School of Automation, Beijing Institute of Technology, Beijing 100081, China.

Color versions of one or more of the figures in this paper are available online at http://ieeexplore.ieee.org.

Digital Object Identifier 10.1109/TIE.2013.2240635

improved prescribed performance function (PPF) that characterizes the convergence rate, maximum overshoot, and steady-state error is proposed and incorporated into the control design. An output error transformed system is derived by applying the PPF on the original system. Consequently, the tracking error of the original system can be guaranteed within the prescribed bound provided the transformed system is stable. For this purpose, an adaptive prescribed performance control (APPC) is designed, which also allows to prove the closed-loop stability. In particular, dynamical friction is explicitly considered by using a newly developed nonlinear continuously differentiable friction model [24], [25]. This model can capture various friction dynamics (e.g., Coulomb, viscous, and Stribeck effects) and has continuous characteristic functions to lead to smooth compensation actions. Then, the friction model is lumped into the NN used for approximating other nonlinear dynamics (e.g., resonances and disturbances); thus, the associated primary parameters are online updated, together with NN weights. As a result, the costly rigorous offline identification of friction is avoided without sacrificing tracking performance. Moreover, in terms of appropriate operations, only a scalar parameter, independent of the number of hidden nodes in the NN, is online updated as NN weight to reduce the computational costs. To validate the efficacy of the proposed control, practical experiments are carried out on a laboratory turntable servo platform. Comparative experimental results reveal that the proposed APPC based on the PPF design and friction compensation outperforms others with regarding to both transient and steady-state performance.

This paper is organized as follows. The problem statement is given in Section II. Section III proposes the adaptive control design and the stability analysis. Section IV presents experiments results. Some conclusions are provided in Section V.

II. Problem Formulation

A. Servo Mechanism

The turntable servo mechanism driven by a dc torque motor can be described as [26]

$$\begin{cases} J\ddot{q} + f(q,\dot{q}) + T_f + T_l + T_d = T_m \\ K_E\dot{q} + L_a\frac{dI_a}{dt} + R_aI_a = u \\ T_m = K_TI_a \end{cases} \tag{1}$$

where q and $\dot{q}$ are the angular position (in radians) and velocity (in radians per second), respectively; J is the inertia (in kg/m^2); $f(q,\dot{q})$ is the unknown resonances and uncertainties; T_d, T_l, T_f, and T_m are the unknown disturbance, load, friction, and the generated torque, respectively; u is the control input voltage; I_a, R_a, and L_a are the armature current, resistance, and inductance, respectively; K_T is the electrical–mechanical conversion constant; and K_E is the back electromotive force coefficient.

In a practical system, if the electrical constant L_a/R_a is small, then the electrical transients L_adI_a/dt is close to zero [17]. We define the system states as $x = [x_1, x_2]^T = [q, \dot{q}]^T$; then, the dynamics of servo mechanism (1) can be simplified as

$$\begin{cases} \dot{x}_1 = x_2 \\ \dot{x}_2 = \frac{1}{J}\left(K_1u - K_2x_2 - f(x_1,x_2) - T_l - T_d - T_f\right) \\ y = x_1 \end{cases} \tag{2}$$

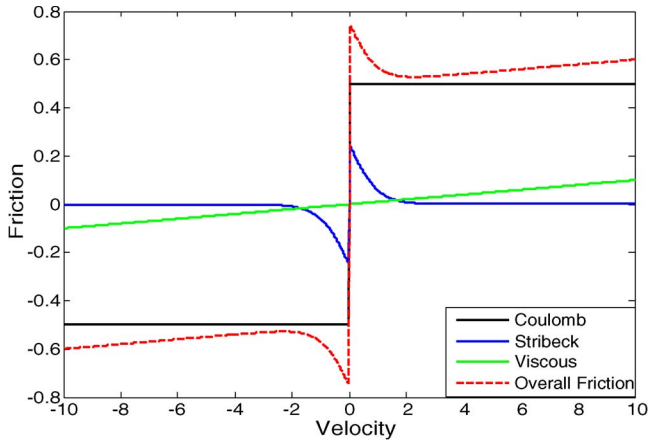

Fig. 1. Profile of friction model (3).

where $K_1 = K_T/R_a$, $K_2v = K_TK_E/R_a$ are positive constants.

The objective of this paper is to derive control u so that:

P1: The output y tracks a given reference y_d, and all signals in the closed-loop are bounded.

P2: Both prescribed transient and steady-state performances of the tracking error $e = y - y_d$ are preserved.

Assumption 1: Position y and velocity $\dot{y}$ are measurable, and the reference y_d, $\dot{y}_d$, and $\ddot{y}_d$ are continuous and bounded.

B. Continuously Differentiable Friction Model

Conventional friction models (e.g., [4]–[7]) are discontinuous or piecewise continuous, which may be problematic for deriving smooth control actions [24]. Moreover, the identification of friction model parameters is not a trivial task. In this paper, a newly developed continuously differentiable friction model [24], [25] is adopted, where the friction torque T_f can be presented as the following parameterized form:

$$T_f = \alpha_1\left(\tanh\left(\beta_1\dot{q}\right) - \tanh\left(\beta_2\dot{q}\right)\right) + \alpha_2\tanh\left(\beta_3\dot{q}\right) + \alpha_3\dot{q} \tag{3}$$

where α_1, α_2, α_3, β_1, β_2, and β_3 are positive parameters.

Unlike other friction models, (3) has a continuously differentiable form to allow more flexible and suitable adaptive control. The static friction coefficients are α_1 and α_2, and the Stribeck effect is captured by $\tanh\left(\beta_1\dot{q}\right) - \tanh\left(\beta_2\dot{q}\right)$. The Coulomb friction is dominated by $\alpha_2\tanh(\beta_3\dot{q})$, and the viscous dissipation is denoted by $\alpha_3\dot{q}$. For further details, we refer to [24]. As for an example, Fig. 1 provides the profile of (3) with $\alpha_1 = 0.25$, $\alpha_2 = 0.5$, $\alpha_3 = 0.01$, $\beta_1 = 100$, $\beta_2 = 1$, and $\beta_3 = 100$. In the subsequent control design, friction model (3) will be merged into an NN, so that offline modeling is successfully avoided. Moreover, the modeling error of (3) can be lumped into the additive disturbance T_d, which will be compensated in the control design.

C. NN Approximation

To approximate unknown nonlinearities, an NN approximator [18] is used over a compact set Ω as

$$Q(Z) = W^T\Phi(Z) + \varepsilon \quad \forall Z \in \Omega \subset \mathbb{R}^n \tag{4}$$

where $Q(Z)$ is the unknown function to be approximated; $W = [w_1, w_2, \ldots, w_L]^T \in \mathbb{R}^L$ is the bounded NN weight vector, and $\varepsilon \in \mathbb{R}$ is a bounded approximation error, i.e., $\|W^*\| \leq W_N$, $|\varepsilon| \leq \varepsilon_N$ with W_N, and ε_N being positive constants. $\Phi(Z) = [\Phi_1(Z), \cdots \Phi_L(Z)]^T \in \mathbb{R}^L$ is the NN basis vector. In this paper, a high-order NN (HONN) [27], [28] with basis functions $\Phi_k(Z) = \prod_{j \in J_k}[\sigma(Z_j)]^{d_k(j)}$, $k = 1, \ldots, L$ are used with J_k being collections of L-nonordered subsets of $\{0, 1, \ldots, n\}$, and $d_k(j)$ being nonnegative integers. $\sigma()$ is a sigmoid function $\sigma(x) = a/(1 + e^{-bx}) + c\ \forall a,\ b \in \mathbb{R}^+,\ c \in \mathbb{R}$, where the positive parameters a, b, and real number c are the bound, slope, and bias of sigmoidal curvature, respectively.

III. Adaptive Control Design

A. Prescribed Performance Function

To study the transient and steady-state performances of tracking error $e(t) = y(t) - y_d(t)$, a positive decreasing smooth function $\mu(t) : \mathbb{R}^+ \to \mathbb{R}^+$ with $\lim_{t\to\infty} \mu(t) = \mu_\infty > 0$ will be used as the PPF. In this paper, we select $\mu(t)$ as

$$\mu(t) = (\mu_0 - \mu_\infty)e^{-\kappa t} + \mu_\infty \tag{5}$$

where $\mu_0 > \mu_\infty$ and $\kappa > 0$ are design parameters.

As presented in [22] and [23], it is sufficient to achieve the control objective P2 if condition (6) holds

$$-\underline{\delta}\mu(t) < e(t) < \overline{\delta}\mu(t) \quad \forall t > 0 \tag{6}$$

where $\underline{\delta}$ and $\overline{\delta} > 0$ are constants selected by the designer.

In (5) and (6), we know that $\overline{\delta}\mu_0$ defines the upper bound of the maximum overshoot and $-\underline{\delta}\mu_0$ defines the lower bound of the undershoot, the decreasing rate κ introduces a lower bound on the convergence speed, and μ_∞ denotes the allowable steady-state tracking error [22]. Hence, the transient and steady-state performances can be designed *a priori* by tuning the parameters $\underline{\delta}$, $\overline{\delta}$, κ, μ_0, and μ_∞.

To solve the control problem with prescribed performance (6), an output error transform will be introduced by transforming condition (6) into an equivalent "unconstrained" one [23]. For this purpose, we define a smooth, strictly increasing function $S(z_1)$ of the transformed error $z_1 \in \mathbb{R}$, such that:

1) $-\underline{\delta} < S(z_1) < \overline{\delta}, \forall z_1 \in L_\infty$.
2) $\lim_{z_1\to+\infty} S(z_1) = \overline{\delta}$, and $\lim_{z_1\to-\infty} S(z_1) = -\underline{\delta}$.

From the properties of $S(z_1)$, condition (6) is equal to

$$e(t) = \mu(t)S(z_1). \tag{7}$$

Since $S(z_1)$ is strictly monotonic increasing and the fact that $\mu(t) \geq \mu_\infty > 0$ holds according to (5), the inverse function of $S(z_1)$ exists and can be deduced as

$$z_1 = S^{-1}\left[\frac{e(t)}{\mu(t)}\right]. \tag{8}$$

Note that PPF (5), $S(z_1)$ and the associated parameters $\underline{\delta}$, $\overline{\delta}$, κ, μ_0, μ_∞, are all *a priori* designed. For any initial condition $e(0)$, if parameters μ_0, $\underline{\delta}$, and $\overline{\delta}$ are selected such that $-\underline{\delta}\mu(0) < e(0) < \overline{\delta}\mu(0)$ and z_1 can be controlled to be bounded (i.e., $z_1 \in L_\infty, \forall t > 0$), then $-\underline{\delta} < S(z_1) < \overline{\delta}$ holds; thus, the condition $-\underline{\delta}\mu(t) < e(t) < \overline{\delta}\mu(t)$ is guaranteed. Consequently, the tracking control problem of system (2) is now transformed to stabilize the transformed system (8).

Lemma 1: The control of system (2) is invariant under the error transform (8) with function $S(z_1)$, fulfilling properties 1 and 2 [23]. Thus, the stabilization of transformed error dynamics z_1 in (8) is sufficient to guarantee the tracking control of system (2) with prescribed error performance (6).

Proof: The proof can be derived based on (6), (7), and (8).

A similar idea for error transform was initially proposed in [22] and [23], where the tracking error was factorized into a more complex structure depending on the initial condition $e(0)$. Here, we introduce parameters $\underline{\delta}$, $\overline{\delta}$, and a unified error function $S(z_1)$ with properties 1 and 2, so that the subsequent control design can be simplified with

$$S(z_1) = \frac{\overline{\delta}e^{z_1} - \underline{\delta}e^{-z_1}}{e^{z_1} + e^{-z_1}}. \tag{9}$$

Then, from (8), the transformed error z_1 is derived as

$$z_1 = S^{-1}\left[\frac{e(t)}{\mu(t)}\right] = \frac{1}{2}\ln\frac{\lambda(t) + \underline{\delta}e^{-z_1}}{\overline{\delta} - \lambda(t)} \tag{10}$$

where $\lambda(t) = e(t)/\mu(t)$.

To stabilize the error system z_1 and thus to achieve the guaranteed performance of error e, we further deduce

$$\begin{aligned}\dot{z}_1 &= \frac{\partial S^{-1}}{\partial\lambda}\dot{\lambda} = \frac{1}{2}\left[\frac{1}{\lambda + \underline{\delta}} - \frac{1}{\lambda - \overline{\delta}}\right]\left(\frac{\dot{e}}{\mu} - \frac{e\dot{\mu}}{\mu^2}\right)\\ &= r(x_2 - \dot{y}_d - e\dot{\mu}/\mu)\end{aligned} \tag{11}$$

where $r = (1/2\mu)[1/(\lambda + \underline{\delta}) - 1/(\lambda - \overline{\delta})]$ can be calculated based on $e(t)$ and $\mu(t)$, and fulfills $0 < r \leq r_M = (\underline{\delta} + \overline{\delta})/(\mu_\infty\underline{\delta}\overline{\delta})$.

Moreover, one may obtain that

$$\begin{aligned}\ddot{z}_1 =& \dot{r}(x_2 - \dot{y}_d - e\dot{\mu}/\mu)\\ &+ r(\dot{x}_2 - \ddot{y}_d - \dot{e}\dot{\mu}/\mu - e\ddot{\mu}\mu/\mu^2 + e\dot{\mu}^2/\mu^2)\\ =& \dot{r}(x_2 - \dot{y}_d - e\dot{\mu}/\mu) - r(\ddot{y}_d + \dot{e}\dot{\mu}/\mu + e\ddot{\mu}\mu/\mu^2 - e\dot{\mu}^2/\mu^2)\\ &+ r\left(\zeta(x) - T_F(x_2) + gu\right)\end{aligned} \tag{12}$$

where $g = K_1/J > 0$ is a positive constant, $T_F(x_2) = T_f/J$ is the friction, and $\zeta(x) = (-K_2x_2 - f(x) - T_l - T_d)/J$ is a nonlinear function including unknown dynamics, disturbances, and the load torque.

Define the filtered error as

$$s = [\,\Lambda \quad 1\,][z_1, \dot{z}_1]^T \tag{13}$$

where $\Lambda > 0$ is a positive constant such that the tracking error z_1 is bounded as long as s is bounded.

Consequently, we have

$$\begin{aligned}\dot{s} =& (\Lambda r + \dot{r})(x_2 - \dot{y}_d - e\dot{\mu}/\mu) + r\left(\zeta(x) - T_F(x_2) + gu\right)\\ &- r(\ddot{y}_d + \dot{e}\dot{\mu}/\mu + e\ddot{\mu}\mu/\mu^2 - e\dot{\mu}^2/\mu^2)\\ =& rF(x, \dot{y}_d, \ddot{y}_d, r, e) - rT_F(x_2) + rgu\end{aligned} \tag{14}$$

where $F(x,\dot{y}_d,\ddot{y}_d,r,e)=\zeta(x)+(\Lambda+\dot{r}/r)(x_2-\dot{y}_d-e\dot{\mu}/\mu)-(\ddot{y}_d+\dot{e}\dot{\mu}/\mu+e\ddot{\mu}\mu/\mu^2-e\dot{\mu}^2/\mu^2)$ denotes the lumped nonlinearities, which are approximated by HONN (4) as

$$F(x,\dot{y}_d,\ddot{y}_d,r,e)=W^T\Phi(Z)+\varepsilon \quad \forall Z=[x,\dot{y}_d,\ddot{y}_d,r,e]\in\mathbb{R}^6. \tag{15}$$

Moreover, according to (3), we can further rewrite the friction dynamics $-T_F(x_2)$ as

$$-T_F(x_2)=\alpha^T\phi(x_2) \tag{16}$$

where $\alpha=[\alpha_1,\alpha_2,\alpha_3]^T$ are the friction coefficients, and $\phi=[-(\tanh(\beta_1x_2)-(\beta_2x_2)),-\tanh(\beta_3x_2),-x_2]^T$ is a vector.

Define $\Theta=[W^T,\alpha^T]^T$ and $\Psi=[\Phi^T,\phi^T]^T$; then, one can represent error equation (14) as

$$\dot{s}=r(\Theta^T\Psi+\varepsilon+gu). \tag{17}$$

Remark 1: In (17), the friction dynamics shown in (16) are lumped into the NN approximation (15), resulting in a more compact form $\Theta^T\Psi$. Moreover, we define an unknown scalar $\theta=\Theta^T\Theta$ as the lumped adaptive parameter of HONN (15) and friction (16), and then a scalar $\hat{\theta}$ (independent of the number of NN nodes), rather than vectors W and α, is updated online in the control, such that the computational costs can be significantly reduced. This is different to conventional NN controllers [18], [19], [21].

B. Adaptive Control Design and Stability Analysis

Control u can be specified as

$$u=-\frac{k_1s}{r}-\frac{\hat{\theta}s}{2\eta^2}\Psi^T\Psi-\frac{\hat{\varepsilon}^2s}{\hat{\varepsilon}|s|+\sigma_1} \tag{18}$$

$$\dot{\hat{\theta}}=r\Gamma\left[\frac{s^2}{2\eta^2}\Psi^T\Psi-\sigma_2\hat{\theta}\right] \tag{19}$$

$$\dot{\hat{\varepsilon}}=r\Gamma_a\left[|s|-\sigma_3\hat{\varepsilon}\right] \tag{20}$$

where $\Gamma>0$, $\Gamma_a>0$, $k_1>0$, $\eta>0$, and σ_1, σ_2, and $\sigma_3>0$ are design parameters.

We have the following result.

Theorem 1: Consider adaptive system comprising system (1) with the error transform (10), control (18) and adaptive laws (19) and (20). Then, the following hold.

1) All signals in the closed-loop system are semi-globally uniformly ultimately bounded.
2) The prescribed control performance (6) is preserved.

Proof: The detailed proof can be found in the Appendix.

C. Practical Implementation

The implementation of the proposed APPC is presented step-by-step as follows.

1) Determine parameters k_1, Γ, Γ_a, σ_1, σ_2, σ_3, μ_0, μ_∞, κ, $\overline{\delta}$, $\underline{\delta}$, and initial condition $\hat{\theta}(0)\geq 0$, $\hat{\varepsilon}(0)\geq 0$.
2) Derive the tracking error $e=y-y_d$ and z_1 and $\dot{z}_1$ based on (10) and (11), and obtain the filtered error (13).
3) Calculate the practical control effort u according to (18), and update the adaptive parameters based on (19) and (20).
4) Apply the derived control on the realistic system and record the input/output measurements.
5) Go back to Step 2 for the next sampling interval.

In practical applications, a preliminary parameter tuning session needs to be conducted. All parameters can be taken into two groups: i) the PPF parameters μ_0, μ_∞, κ, $\underline{\delta}$, and $\overline{\delta}$ mainly determine the control performance and can be selected offline; ii) the control parameters k_1, Γ, Γ_a, σ_1, σ_2, and σ_3 are determined online based on a trial-and-error method to stabilize the transformed error system (14). Here, the detailed tuning guidelines for all parameters are summarized as follows.

1) The PPF parameters μ_0, $\underline{\delta}$, and $\overline{\delta}$ should be selected to ensure $-\underline{\delta}\mu(0)<e(0)<\overline{\delta}\mu(0)$, which depend on the initial condition of each system, i.e., set them adequately large.
2) The parameter κ determines the tracking error convergence speed and thus can be set small at the beginning and then increased via a trial-and-error method. μ_∞ defines the final steady-state error bound, which can be set initially large and then reduced in the subsequent tuning. The final choice of these two parameters should make a tradeoff between the demand of users and the realistic system operation conditions. In a general case, small μ_∞ and large κ will obtain good tracking performance but in the cost of large control actions.
3) A large k_1 will lead to faster error convergence, whereas the resulting control action may be oscillated. High gains Γ and Γ_a will improve the parameter adaptation and, thus, the tracking performance. However, when they are too large, the control action may be aggressive.
4) The parameters σ_2 and σ_3 denote the σ-modification in the adaptive laws [9]. However, large σ_2 and σ_3 will suppress the parameter adaptation speed. Moreover, σ_1 is used to avoid the singularity in control (18) and to guarantee the smoothness of control actions.

Moreover, the structure of HONN is determined by increasing the number of NN nodes until no further improvement of tracking accuracy can be observed.

Remark 2: In the proposed control, the initial condition $-\underline{\delta}\mu(0)<e(0)<\overline{\delta}\mu(0)$ should be guaranteed by designing the PPF parameters μ_0, $\underline{\delta}$, and $\overline{\delta}$, so that $z_1(0)$ is finite. In case z_1 is large (e.g., the output is approaching its bounds), a large control u is derived, which may be stringent due to the hardware limitation. In this case, a possible solution is to reset the control parameters (e.g. large μ_0, $\underline{\delta}$, and $\overline{\delta}$).

IV. Experimental Validation

A. Experimental Setup

To demonstrate the applicability of the proposed method, a turntable motor servo system is employed as the test rig [29] (see Fig. 2), which consists of a permanent-magnet synchronous motor (PMSM, HC-UFS13), an encoder, pulsewidth

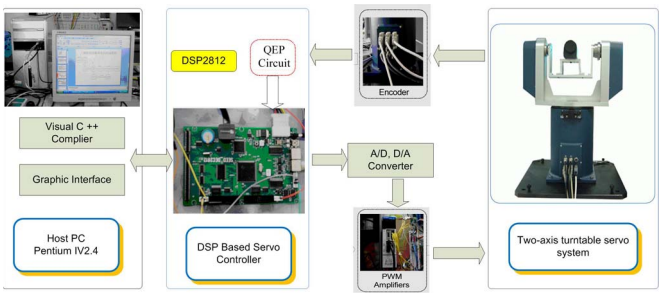

Fig. 2. Diagram of turntable servo test rig.

modulation amplifiers in the motor drive card (MR-J2S-10A), a digital signal processor (DSP, TMS3202812) performing as the controller, and a host Pentium IV 2.8-GHz personal computer operating for display. The proposed control algorithms, including the encoder resolver, are implemented via a C program in CCS3.0 (Compiler CCS3.0 from Texas Instruments) in the DSP. In the tests, the angular position is measured by using an encoder with a resolution of 800 divisions, and the quadrature encoder pulse circuit is used for capturing and converting the speed and position information of the turntable encoders. A gear transmission system with a gear ratio of 80 is included; then, the encoder output signals have a resolution of $800 \times 80 = 64\,000$ per rotation.

This test rig is used to implement the tracking control for given angular position references, where the PMSM is operated in direct torque control mode. In the experiments, only the yaw axis is used, and a sampling rate of 0.01s is selected, which is significantly faster than the later considered closed-loop demand frequencies.

B. Design of Controllers

In this paper, four control methods are compared.

1) APPC: A preliminary tuning session is performed, following the guidelines in Section III-C, to set the PPF parameters $\mu_0 = 0.15$, $\mu_\infty = 0.03$, $\kappa = 0.4$, and $\underline{\delta} = \overline{\delta} = 1$. Then, the control parameters for (18), (19), and (20) are $\Lambda = 15$, $k_1 = 1$, $\Gamma = 0.5$, $\Gamma_a = 0.5$, $\eta = 1$, $\sigma_1 = \sigma_2 = \sigma_3 = 0.01$, and initial condition $\hat{\theta}(0) = 0$, $\hat{\varepsilon}(0) = 0$. The HONN activation function is chosen as $\sigma(x) = 0.5/(1 + e^{-1x}) + 0.1$, and a systematic online tuning leads to the final choice of an NN with $L = 8$.

2) ANC: The adaptive neural control (ANC) with a linear sliding mode term [30] is tested. The control is $u = ks + \hat{W}^T\Phi + u_1$, where $u_1 = \sigma s/|s|$ for $s \neq 0$ or $u_1 = 0$ for $s = 0$ is a sliding mode term, and $s = \Lambda e_1 + e_2$ is the filtered error with $e_1 = y_d - x_1$ and $e_2 = \dot{y}_d - x_2$. The adaptive law is $\dot{\hat{W}} = \Gamma s\Phi$, and the control parameters are $\Lambda = 15$, $k = 1$, $\Gamma = 0.5$, and $\sigma = 0.005$.

3) ANDSC: The adaptive neural DSC proposed in [29] is carried out, where the errors are defined as $z_1 = x_1 - y_d$ and $z_2 = x_2 - s_1$ with $\mu_1\dot{s}_1 + s_1 = \alpha_1$ and $\alpha_1 = -k_1 z_1 - \hat{\theta}_1 z_1 \Phi_1^T\Phi_1/2 - \hat{\varepsilon}_1 \tanh(z_1/\omega_1)$, and the control is $u = -k_2 z_2 - \hat{\theta}_2 z_2 \Phi_2^T\Phi_2/2 - \hat{\varepsilon}_2 \tanh(z_2/\omega_2)$ with adaptive laws $\dot{\hat{\theta}}_i = \Gamma_i[z_i^2\Phi_i^T\Phi_i - \sigma_i\hat{\theta}_i]/2$ and $\dot{\hat{\varepsilon}}_i = \Gamma_a[z_i \tanh(z_i/\omega_i) - \sigma_{ai}\hat{\varepsilon}_i]$. The parameters are $k_1 = 9$, $k_2 = 4$, $\Gamma_1 = \Gamma_2 = 100$, $\mu_1 = 0.01$, $\Gamma_{a1} = \Gamma_{a2} = 10$, $\sigma_1 = \sigma_2 = \sigma_{a1} = \sigma_{a2} = 0.01$, and $\omega_1 = \omega_2 = 1$.

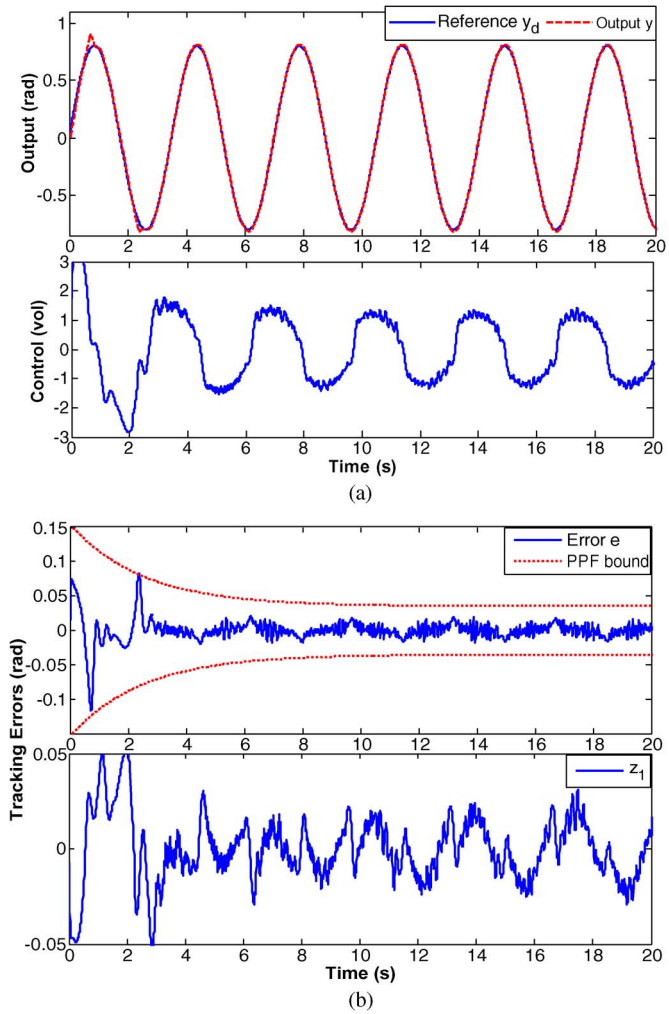

Fig. 3. Control performance of (18) for $y_d = 0.8\sin(2\pi t/3.5)$. (a) Output tracking and control signal. (b) Tracking errors.

4) PID Control: Finally, a PID control is tested for comparison. The PID parameters $K_p = 40$; $K_i = 1$; $K_d = 0.1$ are determined via a heuristic tuning approach for a given position reference, e.g., $q_d(t) = 0.8\sin(0.5\pi t)$, to make a tradeoff between the steady-state performance and transient performance.

C. Experimental Results

For fair comparison, all control parameters are fixed for various reference signals. To compare the control performance quantitatively, four indices are adopted [29]: 1) integrated absolute error IAE $= \int |e(t)|dt$; 2) integrated square error ISDE $= \int (e(t) - e_0)^2 dt$, where e_0 is the mean value of error; 3) integrated absolute control IAU $= \int |u(t)|dt$; and 4) integrated square control ISDU $= \int (u(t) - u_0)^2 dt$, where u_0 is the mean value of the control signal.

1) Case 1—Sinusoidal-Wave Tracking: Sinusoidal waves with various amplitudes and frequencies are first employed as the references. Extensive experiments have been conducted, and two results are shown in Figs. 3 and 4 with control (18), (19) and (20), where the outputs, the control voltages, the tracking errors, and the adaptive parameters are all depicted. Fig. 3 depicts the tracking control for a fast-varying reference

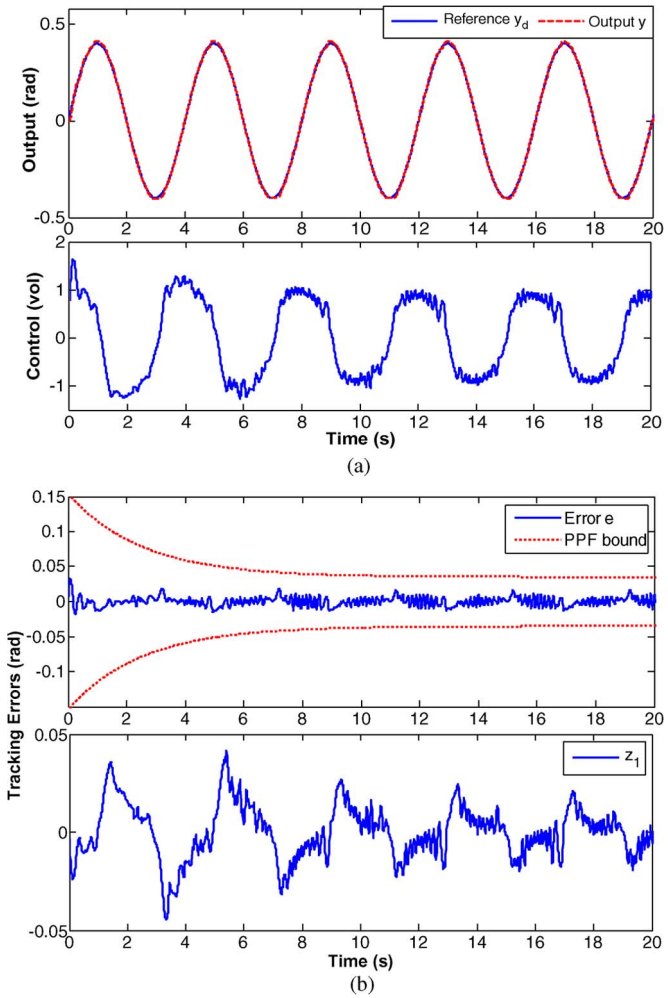

Fig. 4. Control performance of (18) for $y_d = 0.4\sin(2\pi t/4)$. (a) Output tracking and control signal. (b) Tracking errors.

$y_d = 0.8\sin(2\pi t/3.5)$, and Fig. 4 shows the performance for $y_d = 0.4\sin(2\pi t/4)$. It is shown that satisfactory output tracking control is achieved. In particular, the tracking errors are indeed bounded by the designed PPF (6), as shown in Figs. 3(b) and 4(b), which clearly indicates that the proposed prescribed transient and steady-state performances are all retained, as claimed in Theorem 1.

To further show the efficacy and to compare the control performance, Table I summarizes all indices for both sinusoidal references with different amplitudes and periods. From Table I, one can see that the proposed APPC gives smaller IAE and ISDE in all cases and thus better control performance, i.e., it can obtain smaller tracking error. The ANC and ANDSC achieve very similar control performance in terms of IAE and ISDE, whereas ANDSC imposes large control effort (i.e., IAU) and fluctuations (i.e., ISDU). Among all controllers, PID control requires similar control efforts (e.g., IAU and ISDU) and error performance (e.g., IAE and ISDE) to ANC.

2) Case 2—Sinusoidal Waves With Varying Amplitudes: Since the influence of friction nonlinearities are more notable at low speed, to show the compensation for friction, we select a sinusoidal signal $y_d = A\sin(2\pi t/5)$ with a fixed period $T = 5$ s and varying amplitude $A = 0.4{-}1.2$ rad as the reference. The comparative performance is summarized in Table II. It is also found that the proposed APPC performs better than other control schemes due to the introduction of the PPF design and the friction compensation via the continuously differentiable friction model (3). Moreover, in the low-speed regime (e.g., $A = 0.4, 0.6$), ANDSC performs slightly better than ANC, whereas in the middle/high-speed regime (e.g., $A = 0.8 \sim 1.2$), its performance is deteriorated. Among all case studies, PID control gives larger error, which exactly illustrates how the addition of the adaptive element allows for the compensation of time-varying dynamics to improve the overall control performance.

As an example, Fig. 5 depicts the tracking profiles and the corresponding errors for $y_d = 0.4\sin(0.4\pi t)$ with different controllers. One can find in Fig. 5(a) that the proposed APPC can compensate for the dynamics of friction effectively, i.e., it gives smaller tracking errors at the point of maximum amplitude and thus provides smallest error as shown in Fig. 5(b).

3) Case 3—Step Setpoint: To further justify the transient performance (e.g., overshoot), a step reference with amplitude 0.8 rad is used. To fulfill condition $-\underline{\delta}\mu(0) < e(0) < \overline{\delta}\mu(0)$, the PPF is modified as $\mu(t) = (1 - 0.01)e^{-3.5t} + 0.01$ with bounding parameters $\underline{\delta} = 1$ and $\overline{\delta} = 0.2$. Other control parameters are the same as those defined earlier. As shown in Fig. 6, the prescribed performance (6) is retained; in particular, the transient performance is satisfactory compared with other schemes, for which the overshoot reaches or exceeds the prescribed bounds.

All the aforementioned experimental results clearly show that the proposed APPC can retain the prescribed control performance. Moreover, compared with other model-based friction compensations [1], [3], [8], a continuous differentiable friction model with online-updated parameters is adopted so that the time-consuming offline system identification procedure can be avoided and reduced computational costs are imposed. However, this is in the cost of a relatively complex parameter tuning procedure, as summarized in Section III-C.

V. Conclusion

An adaptive control has been proposed for a class of nonlinear mechanisms with guaranteed transient and steady-state tracking performances. The difficulty from the unavoidable friction was circumvented by adopting a new continuously differentiable friction model, which was lumped into the NN for approximating unknown dynamics. A novel HONN with a scalar weight parameter was developed, allowing for reduced computational costs. Consequently, primary friction model parameters were updated together with NN weights to avoid time-consuming and costly rigorous offline identification of friction. Moreover, a PPF and an output error transformation were investigated such that both transient and steady-state performances (e.g., overshoot, convergence speed, and steady-state error) of the tracking error were guaranteed by stabilizing the transformed system. It was shown with experiments that the introduced PPF design and friction compensation improved the control performance.

TABLE I
COMPARISON FOR SINUSOIDAL REFERENCES

	$y_d = 0.4\sin(2\pi t/4)$				$y_d = 0.8\sin(2\pi t/3.5)$			
	PID	ANC	ANDSC	APPC	PID	ANC	ANDSC	APPC
IAE	0.2119	0.2336	0.2029	0.0993	0.4048	0.3055	0.4682	0.1966
ISDE	0.0035	0.0045	0.0041	0.0008	0.0132	0.0093	0.0199	0.0056
IAU	17.089	15.231	15.783	15.263	26.365	26.979	30.234	22.210
ISDU	16.809	13.194	14.200	13.851	60.958	68.324	87.077	30.281

TABLE II
TRACKING PERFORMANCE IAE FOR $y_d = A\sin(0.4\pi t)$

Amplitude (rad)	A=0.4	A=0.6	A=0.8	A=1	A=1.2
PID	0.1998	0.2247	0.3275	0.3325	0.6785
ANC	0.1944	0.1842	0.2184	0.1721	0.3697
ANDSC	0.1347	0.1849	0.2502	0.3249	0.6788
APPC	0.0664	0.0980	0.1024	0.1165	0.2299

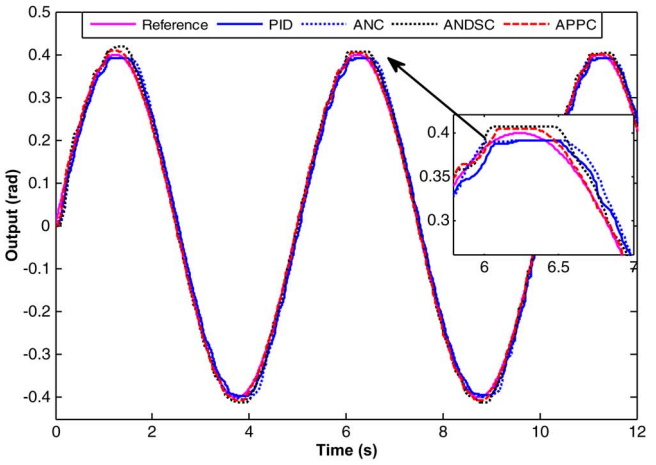

(a)

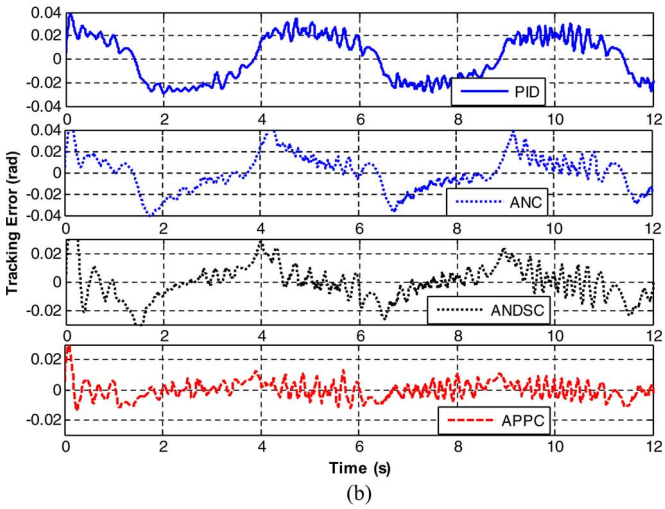

(b)

Fig. 5. Control performance for $y_d = 0.4\sin(0.4\pi t)$. (a) Output profiles. (b) Tracking errors.

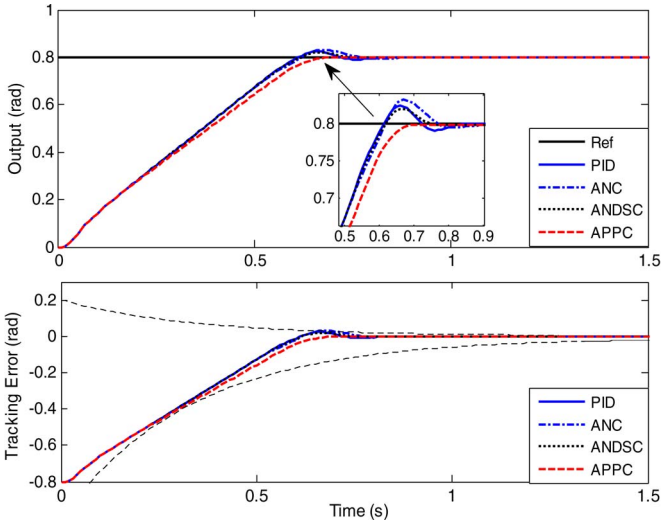

Fig. 6. Control performance for step set point $y_d = 0.8$.

APPENDIX
PROOF OF THEOREM 1

Proof:

1) Select a Lyapunov function as

$$V = \frac{1}{2}s^2 + \frac{g}{2\Gamma}\tilde{\theta}^2 + \frac{g}{2\Gamma_a}\tilde{\varepsilon}^2 \tag{21}$$

where $\tilde{\varepsilon} = \varepsilon^* - \hat{\varepsilon}$ and $\tilde{\theta} = \theta - \hat{\theta}$ are parameter errors between the bounded constants $\varepsilon^* = \varepsilon_N/g$, $\theta = \Theta^T\Theta$ and their estimations $\hat{\varepsilon}$ and $\hat{\theta}$.

The derivative of V along (17)–(20) can be obtained as

$$\begin{aligned}\dot{V} &\le sr\left(\Theta^T\Psi + \varepsilon + gu\right) + \frac{g}{\Gamma}\tilde{\theta}\dot{\tilde{\theta}} + \frac{g}{\Gamma_a}\tilde{\varepsilon}\dot{\tilde{\varepsilon}} \\ &\le sr\Theta^T\Psi + r\varepsilon_N|s| - k_1 g s^2 - \frac{gr\hat{\theta}s^2}{2\eta^2}\Psi^T\Psi - \frac{gr\hat{\varepsilon}^2 s^2}{\hat{\varepsilon}|s| + \sigma_1} \\ &\quad - g\tilde{\theta}r\left[\frac{s^2}{2\eta^2}\Psi^T\Psi - \sigma_2\hat{\theta}\right] - g\tilde{\varepsilon}r\left[|s| - \sigma_3\hat{\varepsilon}\right].\end{aligned} \tag{22}$$

Applying the Young's inequality with $\eta > 0$, one can obtain the following inequalities:

$$sr\Theta^T\Psi \leq \frac{gr\theta s^2}{2\eta^2}\Psi^T\Psi + \frac{r_M\eta^2}{2g} \tag{23}$$

$$\sigma_2 gr\tilde{\theta}\hat{\theta} \leq -\frac{\sigma_2 gr_M\tilde{\theta}^2}{2} + \frac{\sigma_2 gr_M\theta^2}{2} \tag{24}$$

$$\sigma_3 gr\tilde{\varepsilon}\hat{\varepsilon} \leq -\frac{\sigma_3 gr_M\tilde{\varepsilon}^2}{2} + \frac{\sigma_3 gr_M\varepsilon_N^2}{2}. \tag{25}$$

Moreover, it can be verified from (18), (19) and (20) that the fact $\hat{\theta}(t)$, $\hat{\varepsilon}(t) \geq 0$, $t \geq 0$ holds for any initial conditions $\hat{\theta}(0)$, $\hat{\varepsilon}(0) \geq 0$, and $0 \leq ab/(a+b) \leq a\ \forall a, b > 0$ is true. Then, one can rewrite (22) as

$$\begin{aligned}\dot{V} \leq & -k_1 gs^2 + \frac{r_M\eta^2}{2g} + rg\varepsilon^*|s| - rg\tilde{\varepsilon}|s| - \frac{rg\hat{\varepsilon}^2 s^2}{\hat{\varepsilon}|s| + \sigma_1} \\ & + \sigma_2 gr\tilde{\theta}_1\hat{\theta}_1 + \sigma_3 gr\tilde{\varepsilon}\hat{\varepsilon} \\ \leq & -k_1 gs^2 - \frac{\sigma_2 gr_M\tilde{\theta}^2}{2} - \frac{\sigma_3 gr_M\tilde{\varepsilon}^2}{2} + \frac{\sigma_2 gr_M\theta^2}{2} \\ & + \frac{\sigma_3 gr_M\varepsilon_N^2}{2} + \frac{r_M\eta^2}{2g} + \sigma_1 gr_M \\ \leq & -\gamma V + \vartheta \end{aligned} \tag{26}$$

where γ and ϑ are positive constants, i.e.,

$$\gamma = \min\{2k_1 g, \Gamma r_M\sigma_2, \Gamma_a r_M\sigma_3\}$$

$$\vartheta = \sigma_1 gr_M + \sigma_2 gr_M\theta^2/2 + \sigma_3 gr_M\varepsilon_N^2/2 + r_M\eta^2/2g.$$

Then, according to Lyapunov's theorem, V is uniformly ultimately bounded; thus, errors s, $\tilde{\theta}$, and $\tilde{\varepsilon}$ are bounded. This further guarantees the boundedness of the transformed error z_1 and $\dot{z}_1$ according to (13). Moreover, since $\theta = \Theta^T\Theta$ and $\varepsilon^* = \varepsilon_N/g$ are bounded, the adaptive parameters $\hat{\theta}$ and $\hat{\varepsilon}$ are all bounded. Consequently, the control signal u is bounded.

2) We have proven that the transformed error z_1 is bounded, i.e., $z_1 \in L_\infty$. Then, according to the properties of function $S(z_1)$, we know that $-\underline{\delta} < S(z_1) < \overline{\delta}$, which further implies $-\underline{\delta}\mu(t) < e(t) < \overline{\delta}\mu(t)$ according to (7). Then, one can conclude based on Lemma 1 that tracking control of system (2) with prescribed error performance (6) is achieved. □

REFERENCES

[1] G. Tao and F. L. Lewis, *Adaptive Control of Nonsmooth Dynamic Systems*. Berlin, Germany: Springer-Verlag, 2001.

[2] J. Na, G. Herrmann, and X. M. Ren, "Neural network control of nonlinear time-delay system with unknown dead-zone and its application to a robotic servo system," *Trends Intell. Robot.*, vol. 103, pp. 338–345, 2010.

[3] H. Olsson, K. J. Astromm, C. Canudas de Wit, M. Gafvert, and P. Lischinsky, "Friction models and friction compensation," *Eur. J. Control*, vol. 4, no. 3, pp. 176–195, 1998.

[4] J. Amin, B. Friedland, and A. Harnoy, "Implementation of a friction estimation and compensation technique," *IEEE Control Syst. Mag.*, vol. 17, no. 4, pp. 71–76, Aug. 1997.

[5] B. Armstrong-Helouvry, P. Dupont, and C. C. De Wit, "A survey of models, analysis tools and compensation methods for the control of machines with friction," *Automatica*, vol. 30, no. 7, pp. 1083–1138, Jul. 1994.

[6] P. R. Dahl, "A solid friction model," DTIC, Fort Belvoir, VA, USA, Tech. Rep. DTIC Doc. ADA041920, May 1968.

[7] C. Canudas de Wit, H. Olsson, K. J. Astrom, and P. Lischinsky, "A new model for control of systems with friction," *IEEE Trans. Autom. Control*, vol. 40, no. 3, pp. 419–425, Mar. 1995.

[8] Z. Jamaludin, H. Van Brussel, and J. Swevers, "Friction compensation of an XY feed table using friction-model-based feedforward and an inverse-model-based disturbance observer," *IEEE Trans. Ind. Electron.*, vol. 56, no. 10, pp. 3848–3853, Oct. 2009.

[9] P. A. Ioannou and J. Sun, *Robust Adaptive Control*. Englewood Cliffs, NJ, USA: Prentice-Hall, 1996.

[10] S. S. Ge, T. H. Lee, and S. X. Ren, "Adaptive friction compensation of servo mechanisms," *Int. J. Syst. Sci.*, vol. 32, no. 4, pp. 523–532, Apr. 2001.

[11] K. Z. Tang, S. N. Huang, K. K. Tan, and T. H. Lee, "Combined PID and adaptive nonlinear control for servo mechanical systems," *Mechatronics*, vol. 14, no. 6, pp. 701–714, Jul. 2004.

[12] S. Li and Z. Liu, "Adaptive speed control for permanent-magnet synchronous motor system with variations of load inertia," *IEEE Trans. Ind. Electron.*, vol. 56, no. 8, pp. 3050–3059, Aug. 2009.

[13] L. Xu and B. Yao, "Adaptive robust precision motion control of linear motors with negligible electrical dynamics: Theory and experiments," *IEEE/ASME Trans. Mechatronics*, vol. 6, no. 4, pp. 444–452, Dec. 2001.

[14] C. Hu, B. Yao, and Q. Wang, "Adaptive robust precision motion control of systems with unknown input dead-zones: A case study with comparative experiments," *IEEE Trans. Ind. Electron.*, vol. 58, no. 6, pp. 2454–2564, Jun. 2011.

[15] Z. J. Yang, H. Tsubakihara, S. Kanae, K. Wada, and C. Y. Su, "A novel robust nonlinear motion controller with disturbance observer," *IEEE Trans. Control Syst. Technol.*, vol. 16, no. 1, pp. 137–147, Jan. 2008.

[16] G. Zhang, J. Chen, and Z. Lee, "Adaptive robust control for servo mechanisms with partially unknown states via dynamic surface control approach," *IEEE Trans. Control Syst. Technol.*, vol. 18, no. 3, pp. 723–731, May 2010.

[17] G. Zhang, J. Chen, and Z. Li, "Identifier-based adaptive robust control for servomechanisms with improved transient performance," *IEEE Trans. Ind. Electron.*, vol. 57, no. 7, pp. 2536–2547, Jul. 2010.

[18] X. M. Ren, F. L. Lewis, and J. Zhang, "Neural network compensation control for mechanical systems with disturbances," *Automatica*, vol. 45, no. 5, pp. 1221–1226, May 2009.

[19] C. Y. Lai, F. L. Lewis, V. Venkataramanan, X. M. Ren, S. S. Ge, and T. Liew, "Disturbance and friction compensations in hard disk drives using neural networks," *IEEE Trans. Ind. Electron.*, vol. 57, no. 2, pp. 784–792, Feb. 2010.

[20] F. J. Lin and P. H. Chou, "Adaptive control of two-axis motion control system using interval type-2 fuzzy neural network," *IEEE Trans. Ind. Electron.*, vol. 56, no. 1, pp. 178–193, Jan. 2009.

[21] D. Naso, F. Cupertino, and B. Turchiano, "Precise position control of tubular linear motors with neural networks and composite learning," *Control Eng. Pract.*, vol. 18, no. 5, pp. 515–522, May 2010.

[22] C. P. Bechlioulis and G. A. Rovithakis, "Robust adaptive control of feedback linearizable MIMO nonlinear systems with prescribed performance," *IEEE Trans. Autom. Control*, vol. 53, no. 9, pp. 2090–2099, Oct. 2008.

[23] C. P. Bechlioulis and G. A. Rovithakis, "Adaptive control with guaranteed transient and steady state tracking error bounds for strict feedback systems," *Automatica*, vol. 45, no. 2, pp. 532–538, 2009.

[24] C. Makkar, W. E. Dixon, W. G. Sawyer, and G. Hu, "A new continuously differentiable friction model for control systems design," in *Proc. IEEE/ASME Int. Conf. Adv. Intell. Mechatron.*, 2005, pp. 600–605.

[25] C. Makkar, G. Hu, W. G. Sawyer, and W. E. Dixon, "Lyapunov-based tracking control in the presence of uncertain nonlinear parameterizable friction," *IEEE Trans. Autom. Control*, vol. 52, no. 10, pp. 1988–1994, Oct. 2007.

[26] K. K. Tan, S. N. Huang, H. F. Dou, T. H. Lee, S. J. Chin, and S. Y. Lim, "Adaptive robust motion control for precise trajectory tracking applications," *ISA Trans.*, vol. 40, no. 1, pp. 57–71, 2001.

[27] E. B. Kosmatopoulos, M. M. Polycarpou, M. A. Christodoulou, and P. A. Ioannou, "High-order neural network structures for identification of dynamical systems," *IEEE Trans. Neural Netw.*, vol. 6, no. 2, pp. 422–431, Mar. 1995.

[28] J. Na, X. M. Ren, and D. Zheng, "Adaptive control for nonlinear pure-feedback systems with high-order sliding mode observer," *IEEE Trans. Neural Netw. Learn. Syst.*, vol. 24, no. 3, pp. 370–382, Mar. 2013.

[29] J. Na, X. M. Ren, G. Herrmann, and Z. Qiao, "Adaptive neural dynamic surface control for servo systems with unknown dead-zone," *Control Eng. Pract.*, vol. 19, no. 11, pp. 1328–1343, Aug. 2011.

[30] L. Wang, T. Chai, and L. Zhai, "Neural-network-based terminal sliding-mode control of robotic manipulators including actuator dynamics," *IEEE Trans. Ind. Electron.*, vol. 56, no. 9, pp. 3296–3304, Sep. 2009.

Jing Na received the B.S. and Ph.D. degrees from the School of Automation, Beijing Institute of Technology, Beijing, China, in 2004 and 2010, respectively.

In 2008, he was a Visiting Student with the Technical University of Catalonia, Barcelona, Spain. From 2008 to 2009, he was a Research Collaborator with the Department of Mechanical Engineering, University of Bristol, Bristol, U.K. Since 2010, he has been with the Faculty of Mechanical and Electrical Engineering, Kunming University of Science and Technology, Kunming, China. His current research interests include adaptive control, time-delay systems, neural networks, parameter estimation, repetitive control, and nonlinear control and applications.

Dr. Na was a Postdoctoral Fellow with the ITER Organization, Cadarache, France, from 2011 to 2012.

Qiang Chen received the B.S. degree in measurement and control technology and instrumentation from Hebei Agricultural University, Baoding, China, in 2002 and the Ph.D. degree in control science and engineering from Beijing Institute of Technology, Beijing, China, in 2012.

He is currently a Lecturer with the College of Information Engineering, Zhejiang University of Technology, Hangzhou, China. His research interests include support vector machines, neural network control, and adaptive control with applications to motion control.

Xuemei Ren received the B.S. degree from Shandong University, Shandong, China, in 1989, and the M.S. and Ph.D. degrees in control engineering from Beijing University of Aeronautics and Astronautics, Beijing, China, in 1992 and 1995, respectively.

She is currently a Professor with the School of Automation, Beijing Institute of Technology, Beijing, China. Her research interests include intelligent systems, neural networks, and adaptive and process control.

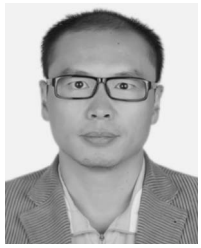

Yu Guo received the B.S. and M.S. degrees from Kunming University of Science and Technology, Kunming, China, in 1993 and 1996, respectively, and the Ph.D. degree in mechanical engineering from Chongqing University, Chongqing, China, in 2003.

He is currently a Professor with the Faculty of Mechanical and Electrical Engineering, Kunming University of Science and Technology. His current research interests include signal processing methods with application to rotating machinery and blind-source separation methods on mechanical vibrations.